Check for updates

Crystal Engineering Hot Paper

How to cite: *Angew. Chem. Int. Ed.* **2022,** *61,* e202206249
International Edition: doi.org/10.1002/anie.202206249
German Edition: doi.org/10.1002/ange.202206249

Topochemical, Single-Crystal-to-Single-Crystal [2+2] Photocycloadditions Driven by Chalcogen-Bonding Interactions

*Jan Alfuth, Olivier Jeannin, and Marc Fourmigué**

Abstract: The face-to-face association of (*E*)-1,2-di(4-pyridyl)ethylene (**bpen**) molecules into rectangular motifs stabilized for the first time by chalcogen bonding (ChB) interactions is shown to provide photoreactive systems leading to cyclobutane formation through single-crystal-to-single-crystal [2+2] photodimerizations. The chelating chalcogen bond donors are based on original aromatic, *ortho*-substituted bis(selenocyanato)benzene derivatives **1**–**3**, prepared from *ortho*-diboronic acid bis(pinacol) ester precursors and SeO_2 and malononitrile in 75–90 % yield. The very short *intramolecular* Se···Se distance in **1**–**3** (3.22–3.24 Å), a consequence of a strong intramolecular ChB interaction, expands to 3.52–3.54 Å in the chalcogen-bonded adducts with **bpen**, a distance (<4 Å) well adapted to the face-to-face association of the **bpen** molecules into the reactive position toward photochemical dimerization.

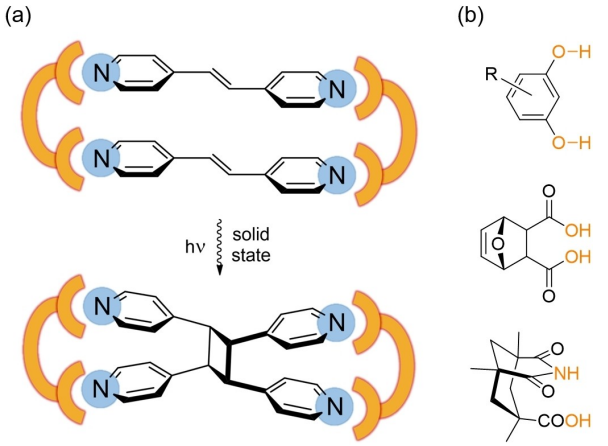

Scheme 1. a) Templated photodimerization of **bpen** in molecular rectangles. b) Examples of ditopic hydrogen bond donors used toward the formation of such molecular rectangles.

Noncovalent interactions have been used in the last years to direct the solid-state organization of reactive molecules toward topochemical reactions under external stimuli such as light or heat.[1] This strategy has been applied with success with olefins when using pincer-like auxiliary molecules or templates to organize them in a face-to-face arrangement suitable for [2+2] cycloaddition under UV irradiation.[2] One prototypical example is the association of (*E*)-1,2-di(4-pyridyl)ethylene (**bpen**) with rigid ditopic templates able to interact with the pyridinyl nitrogen atoms through hydrogen bonding interactions[3] (Scheme 1) or metal coordination.[4]

Under UV irradiation, the corresponding cyclobutane is formed, rarely in a single-crystal-to-single-crystal (SCSC) transformation.[5] In many examples, the template is designed as to present two parallel interaction sites to favor the formation of rectangular motifs of 2:2 stoichiometry, with the **bpen** molecules facing each other at a distance short enough (<4 Å) to favor the [2+2] cycloaddition under irradiation.[6] This strategy was recently extended to σ-hole interactions such as halogen bonding, as shown in Scheme 2.[7] Here the two halogenated (X=I, Br, Cl) aryl groups are either linked together in the proper geometry through covalent bonds or through intermolecular π–π interactions.

Besides halogen bonding, chalcogen bonding (ChB) has been also the subject of recent investigations for applications in crystal engineering.[8] We can mention first the association of strong ChB donor and acceptor sites on the same molecule, as in 1,2,5-telluradiazoles,[9] 1,2-chalcogenazole *N*-oxides,[10,11] benzo-1,3-chalcogenazoles,[12] leading to the formation of infinite ribbons[9,13] or discrete supramolecular assemblies.[14] *Bidentate* chelating molecules bearing two

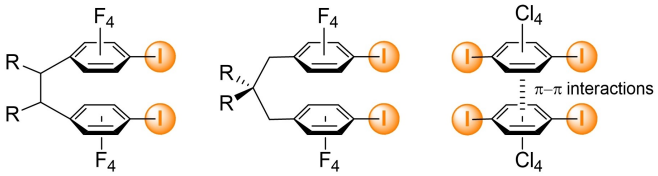

Scheme 2. Examples of ditopic halogen bond donors used toward the formation of molecular rectangles with **bpen**, and exhibiting [2+2] cycloaddition under UV irradiation.

[*] J. Alfuth, Dr. O. Jeannin, Dr. M. Fourmigué
Univ Rennes, CNRS, ISCR (Institut des Sciences Chimiques de Rennes)
35000 Rennes (France)
E-mail: marc.fourmigue@uni-rennes1.fr
J. Alfuth
Department of Organic Chemistry, Faculty of Chemistry, Gdańsk University of Technology
80-233 Gdańsk (Poland)

© 2022 The Authors. Angewandte Chemie International Edition published by Wiley-VCH GmbH. This is an open access article under the terms of the Creative Commons Attribution Non-Commercial NoDerivs License, which permits use and distribution in any medium, provided the original work is properly cited, the use is non-commercial and no modifications or adaptations are made.

© 2022 The Authors. Angewandte Chemie International Edition published by Wiley-VCH GmbH

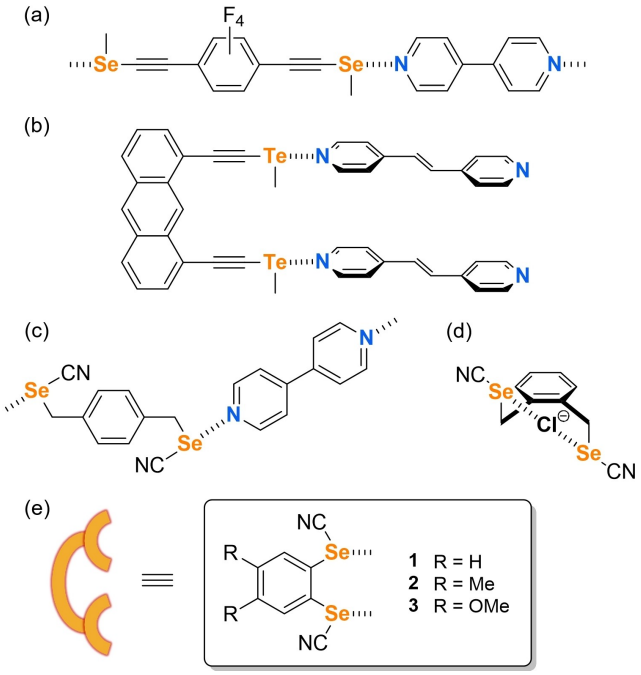

Scheme 3. Activation of σ-hole on selenium atoms and ChB formation with: a), b) alkynyl (chalcogenomethyl), c), d) selenocyanate derivatives and e) targeted ChB donors **1–3**.

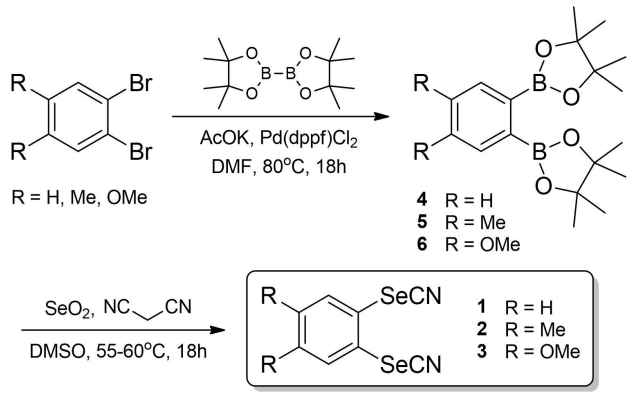

Scheme 4. Synthetic route to the *ortho*-bis(selenocyanato) derivatives **1–3**.

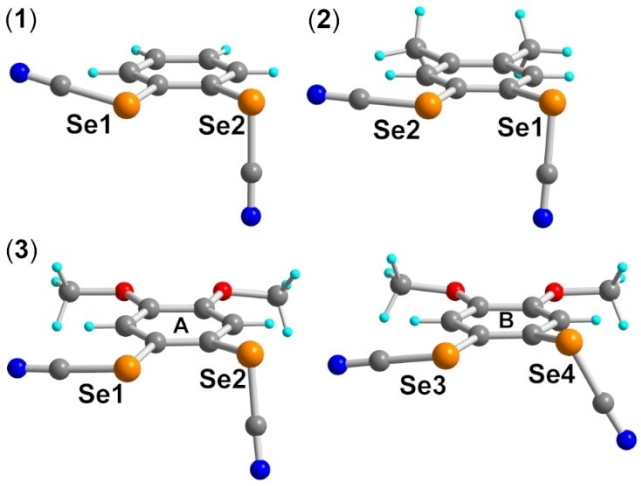

Figure 1. Details of the crystal structures of **1–3**. Note the two crystallographically independent molecules (A, B) in **3**. Intramolecular Se···Se distances amount to 3.245(1) Å in **1**, 3.237(1) Å in **2**, and 3.216(6) and 3.221(7) Å in **3**A and **3**B respectively.

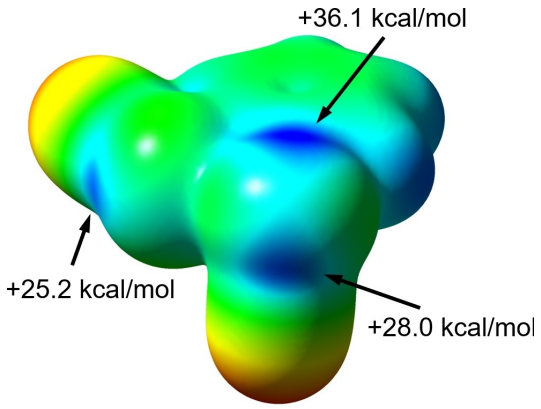

Figure 2. Electrostatic potential (ESP) surface (plotted on the 0.002 e bohr^{-3} isosurface of the electronic density) for compound **1**. Color range from −37.7 (red) to +43.9 (blue) kcal mol^{-1}.

activated chalcogen atoms, but able to interact with one *single* Lewis base, have been also reported in organocatalysis[15,16] or anion recognition[17,18] processes, as in molecules linking two tellurophenes,[19] two 5-(methylchalcogeno)-1,2,3-triazole moieties,[20] two thiophene units,[21] or two selenocyanate groups.[22] Another efficient ChB activation has been reported in chalcogenoacetylenes shown in Scheme 3a-b but co-crystal formation with **bpen** was either unsuccessful or led to structures which appear unreactive under irradiation.[23,24] Considering the efficiency of benzylic selenocyanates (Scheme 3c-d) to engage in ChB interaction with pyridines,[25] we turned our attention to more rigid derivatives and considered aromatic selenocyanates **1–3** as possible linkers to favor the face-to-face association of **bpen**, with possibly a topochemical [2+2] reactivity under irradiation. We report here the synthesis of original organic bis(selenocyanato)benzene derivatives **1–3** and their ability to form cocrystals with **bpen** through strong NC–Se···N_{bpen} chalcogen bond interactions. The proper orientation of the photoreactive **bpen** molecules allows them to enter into efficient [2+2] cycloaddition reactions under UV-irradiation, while also keeping their single-crystal quality.

The preparation of aromatic selenocyanates is usually based on the reaction of KSeCN with either diazonium salts[26] or more electrophilic diaryliodonium salts,[27] both methods suffering from several drawbacks. More recently, the *ipso*-functionalization of arylboronic acids has been reported to afford aryl selenocyanates in good yields, using either SeO_2 and malononitrile,[28] or Se powder with TMS–CN.[29] Both procedures were developed however only with *mono* boronic acids, affording the corresponding

© 2022 The Authors. Angewandte Chemie International Edition published by Wiley-VCH GmbH

MOST WIEDZY Downloaded from mostwiedzy.pl

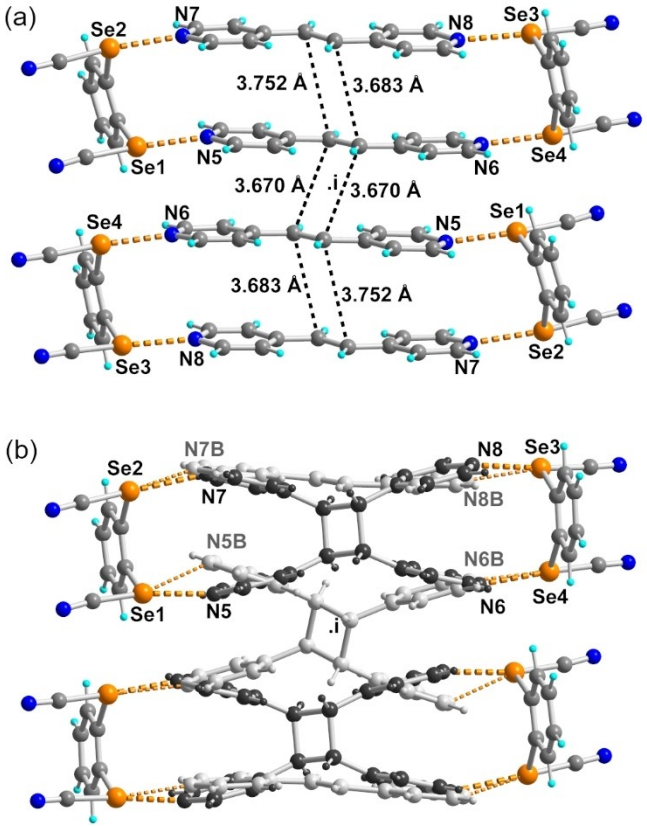

Figure 3. a) Details of the solid-state association of rectangular, chalcogen-bonded motifs in $(\mathbf{1})_4(\mathbf{bpen})_5$. ChB are indicated by orange dotted lines, and short C···C contact between ethylenic moieties by black dotted lines. b) Details of the solid-state association after UV-irradiation and formation of the cyclobutane adducts. Occupation parameters for the two components (shown with atoms in black and light grey) are 0.661(6) and 0.339(6).

mono-selenocyanato derivatives. For the preparation of the desired disubstituted *ortho*-bis(selenocyanato)benzene derivatives **1–3**, we adapted the first procedure (SeO_2/malononitrile) to *ortho*-substituted diboronic derivatives. The preparation of the *ortho*-diboronic acids normally involves the preparation of intermediate boronic ester through lithiation of *ortho*-halogenated aryls, reaction with trimethyl or tri(isopropyl)borane and hydrolysis with HCl.[30] To avoid the isolation and manipulation of the free boronic acids, we considered a modification of reported procedures, performing the selenocyanation reaction directly on boronic esters such as the *ortho*-diboronic acid bis(pinacol) esters **4–6** (Scheme 4). Their preparation involves a Miyaura borylation reaction, adapted from the procedure reported earlier[30b] by replacing the *iso*-propoxy(pinacol)borane with bis(pinacolato)diborane, while using the same experimental conditions (AcOK in anhydrous DMF at 80 °C with Pd(dppf)Cl_2 as catalyst). Under these conditions, the precursors **4–6** were isolated in 50–60 % yields, while the following selenocyanation reaction successfully afforded **1–3** in 75–90 % yields.

All three compounds were purified by chromatography and recrystallized to afford crystals amenable to single-crystal X-ray diffraction. As shown in Figure 1, they all exhibit a recurrent intramolecular chalcogen-bonded motif, with one NC–Se moiety coplanar with the benzene ring and pointing toward a lone pair of the neighboring Se atom, belonging to the second SeCN moiety, which is essentially perpendicular to the benzene ring. The intramolecular Se···Se distances lie in the range 3.22–3.24 Å, notably shorter than the contact distance at 3.80 Å, and corresponding to a reduction ratio (RR) of 3.23 Å/3.80 Å = 0.85.

In order to rationalize this behavior and the solid-state organization (see below) of the three compounds, electrostatic potential (ESP) surfaces were calculated for **1–3** (Figure S1, Table S2 in Supporting Information) and shown in Figure 2 for compound **1**. On the SeCN moiety perpendicular to the benzene ring, we observe two σ-holes (in blue), the strongest one ($+36.1\ kcal\,mol^{-1}$) as anticipated in the prolongation of the NC–Se bond, and a weaker but non-negligible one ($+28.0\ kcal\,mol^{-1}$) in the prolongation of the C_{Ar}–Se bond, as on the other selenocyanate group ($+25.2\ kcal\,mol^{-1}$). Moving to the methyl- and methoxy-substituted derivatives **2** and **3**, these values are slightly decreased (see Table S2 in Supporting Information), as a consequence of the electron-releasing nature of the Me and OMe substituents.

Table 1: Structural characteristics of the ChB interactions in $(\mathbf{1})_4(\mathbf{bpen})_5$, before and after UV irradiation.

ChB	ChB length [Å]	RR	ChB angle [°]
Before irradiation			
NC–Se1···N5	2.670(3)	0.77	175.83(9)
NC–Se2···N7	2.754(4)	0.80	173.58(9)
NC–Se3···N8	2.759(4)	0.75	178.27(9)
NC–Se4···N6	2.656(4)	0.77	175.42(9)
After UV irradiation, major component			
NC–Se1···N5	2.727(11)	0.79	170.52(43)
NC–Se2···N7	3.017(14)	0.87	179.50(52)
NC–Se3···N8	2.649(15)	0.77	175.38(50)
NC–Se4···N6	2.732(12)	0.79	176.38(54)
After UV irradiation, minor component			
NC–Se1···N5B	2.682(21)	0.78	165.08(57)
NC–Se2···N7B	2.640(25)	0.77	174.57(71)
NC–Se3···N8B	2.850(26)	0.83	172.55(66)
NC–Se4···N6B	2.990(23)	0.87	178.27(63)

© 2022 The Authors. Angewandte Chemie International Edition published by Wiley-VCH GmbH

MOST WIEDZY Downloaded from mostwiedzy.pl

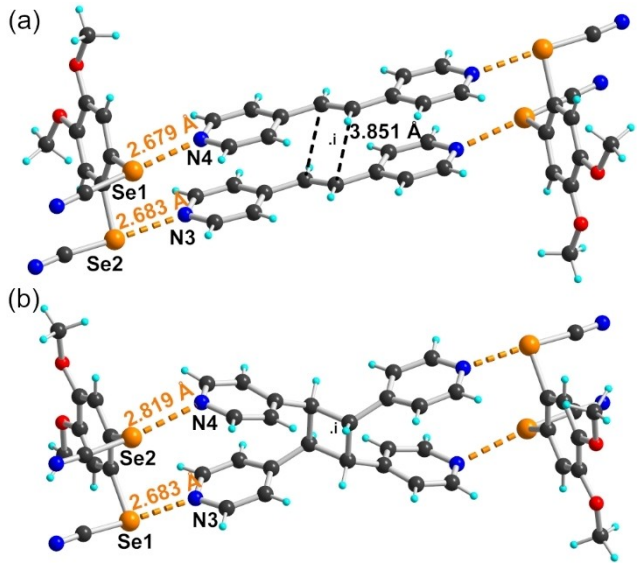

Figure 4. a) Details of the solid-state association within a rectangular chalcogen-bonded motif in (**3**)(**bpen**)$_2$. ChB are indicated by orange dotted lines, and short C···C contact between ethylenic moieties by black dotted lines. b) Details of the solid-state association of the same motif, after UV-irradiation and formation of the cyclobutane ring.

The solid-state organization of the three compounds (see Figures S2–S4 and Table S3 in Supporting Information) is indeed based essentially on a complex set of chalcogen bonding interactions involving these three "free" σ-holes on the two Se atoms as ChB donors and, as ChB acceptors, either the selenium atom of neighboring molecules, the nitrogen lone pairs of nitriles, or the oxygen atoms of the methoxy groups in **3**. The shortest *intermolecular* Se···N and Se···Se distances are associated with a reduction ratio vs. the van der Waals contact distances in the range of 0.85–0.90, comparable with those reported in other organic selenocyanates.[31,32] The main difference to the large set of *benzylic* selenocyanates reported so far is the notably larger σ-hole in the prolongation of the C_{Ar}–Se bond in **1**–**3**, when compared with that found along $ArCH_2$–Se bonds in benzylic selenocyanates.

Elaboration of co-crystals of **1**–**3** with **bpen** was realized by cooling and/or slow evaporation of equimolar quantities of both components in AcOEt. While **1** and **3** gave co-crystals with the desired rectangular motifs (see below), cocrystal with compound **2** crystallizes in the *P*-1 space group as a water solvate with a 2:3 stoichiometry, i.e. with a formulation (**2**)$_2$(**bpen**)$_3$·H_2O, with one **2** and one **bpen** molecule in general position, and another **bpen** and water molecule on inversion centers, associated with each other not only by chalcogen bonding but also hydrogen bonding with the water molecule (See Figure S5 and Table S4 in Supporting Information). This compound does not present a favorable relative orientation of the **bpen** molecules for possible [2+2] cycloaddition and will not be discussed further here.

Co-crystal of **1** with **bpen** crystallizes in the triclinic *P*-1 space group, with a 4:5 stoichiometry, i.e. a formulation (**1**)$_4$(**bpen**)$_5$, with two crystallographically independent **1** molecules, two crystallographically independent **bpen** molecules, and one extra **bpen**$_{dis}$ molecule disordered on an inversion center. The co-crystal can be described as an alternation of layers along *b*, with one layer at $y=0$ incorporating the **bpen**$_{dis}$ and molecules **1**, and one layer at $y=\frac{1}{2}$ with the other **bpen** molecules (Figure S6). The solid-state organization (Figure 3a) is characterized by the association of four **bpen** molecules into tetrameric units, linked together by short Se···N_{bpen} ChBs (Table 1) and small RR values in the range of 0.75–0.80. The remaining **bpen**$_{dis}$ molecule is involved in weaker C–H···N_{bpen} hydrogen bonds. We already note that the *intramolecular* Se···Se chalcogen bonds observed in the ChB donors **1**–**3** alone (see above Figure 1) have been overridden by the stronger ChB with the **bpen** nitrogen atoms, leading to the formation of the desired rectangular boxes, with face-to-face association of **bpen** molecules within the box and intermolecular C···C distances of 3.683(10) and 3.752(10) Å (Figure 3a). Furthermore, two neighboring boxes are related by inversion center and also allow for a face-to-face association of **bpen** molecules, at even shorter intermolecular C···C distance of 3.670(9) Å. Both **bpen** contact lengths are well below the Schmidt rules (<4 Å) for [2+2] cycloaddition.[6]

UV-irradiation of single crystals of (**1**)$_4$(**bpen**)$_5$ provided indeed a single-crystal-to-single-crystal transformation. As shown in Figure 3b, refinement of the crystal structure of the cyclized compound showed, besides the unreacted **bpen**$_{dis}$ molecule disordered on an inversion center, two components with occupation parameters at 0.661(6) and 0.339(6), corresponding to a 2/3–1/3 statistical distribution expected if the [2+2] reactivity within a rectangular box is the same as the reactivity of inversion-related **bpen** molecules between the boxes, which leaves the two outer **bpen** molecules unreacted. This striking behavior is, to our knowledge, completely new, and can be compared only with another example of tetrameric association of **bpen** molecules

Table 2: Structural characteristics of the ChB interactions in (**3**)(**bpen**)$_2$, before and after UV irradiation.

ChB	ChB length [Å]	RR	ChB angle [°]
Before irradiation			
NC–Se1···N4	2.679(7)	0.78	178.88(6)
NC–Se2···N3	2.683(7)	0.78	177.16(6)
After UV irradiation			
NC–Se1···N3	2.863(19)	0.83	176.2(4)
NC–Se2···N4	2.819(18)	0.82	172.2(3)

© 2022 The Authors. Angewandte Chemie International Edition published by Wiley-VCH GmbH

MOST WIEDZY Downloaded from mostwiedzy.pl

linked through hydrogen bonding by indolocarbazole, but in that case only the inner **bpen** molecules reacted with each other.[33] It also demonstrates that the ChB interactions provided by this motif of two selenocyanate moieties in *ortho* position are robust enough to force the face-to-face association of the **bpen** molecules and to stand the severe deformations induced by the photocyclization. Indeed, the small RR values before cyclization (Cf. Table 1) observed in the range 0.75–0.80 (Figure 3a) and characteristic of strong ChB, increase to only 0.77–0.87 in the photo-cyclized products (Figure 3b).

The success of this approach is further confirmed in the co-crystal obtained with the dimethoxy-substituted ChB donor **3** and **bpen**. It crystallizes indeed in the triclinic system, space group *P*-1, with one ChB donor **3** and two **bpen** molecules, all in general position, corresponding to a 1:2 stoichiometry, better described as inversion centered rectangular motifs $(\mathbf{3})_2(\mathbf{bpen})_2$, separated from each other by extra **bpen** molecules (Figure S7).

Within the rectangular motifs (Figure 4a), the **bpen** molecules are associated in a face-to-face manner through ChB with **3** through strong and linear NC–Se···N_{bpen} interactions (Table 2). Contacts between the ethylenic carbon atoms of **bpen** molecules [3.851(7) Å] are longer than those observed in $(\mathbf{1})_4(\mathbf{bpen})_5$ (3.67–3.75 Å), nevertheless shorter than the 4 Å limit. Indeed, UV-irradiation of single crystals of $(\mathbf{3})(\mathbf{bpen})_2$ led to single-crystal-to-single-crystal transformation (Figure 4b), with the desired cyclobutane formation while the other **bpen** molecule interspersed between the rectangles stays unmodified (Figure S8). The ChB interactions (Table 2) are slightly elongated during the photochemical transformation, with RR values evolving from 0.78 to 0.82–0.83.

In conclusion, we have unraveled here for the first time the use of *chalcogen bond* donors such as **1** and **3** to assemble photoreactive **bpen** molecules into face-to-face dimers, allowing for rare single-crystal-to-single-crystal transformations, with the added originality of the striking reactivity of the tetrameric motif isolated with **1**. The structural adaptability of this *ortho*-substituted bis(selenocyanato) motif is highlighted by the evolution of the intramolecular Se···Se distance, from the short 3.22–3.24 Å values in the molecules alone (cf. Figure 1) due to a strong *intramolecular* Se···Se ChB, to a notably larger distance of 3.52–3.54 Å in the chalcogen-bonded adducts with **bpen**, well adapted for the face-to-face association of the **bpen** molecules into reactive position toward photochemical dimerization and cyclobutane formation. Furthermore, as already illustrated by the numerous hydrogen-bonded systems derived from resorcinol derivatives (Scheme 1b),[1–4,7] the three different substitution patterns explored here (R = H, Me, OMe) on the 4,5 positions of the aryl ring let us anticipate many other possibilities by varying the nature of these substituents on all four 3-, 4-, 5- and 6-positions of the benzene ring. We are now focused on exemplifying this structuring motif to other photo- or thermo-reactive molecules with chalcogen bond acceptor capability, toward the elaboration of novel materials with optical or conducting properties.

Acknowledgements

We thank ANR (Paris) for financial support under grant ANR-17-CE07-0025-02. This work has been also supported by the Integrated Development Program of the Gdańsk University of Technology program No. POWR.03.05.00-00.Z044/17 funded by the European Social Fund under the Knowledge Education Development Operational Program.

Conflict of Interest

The authors declare no conflict of interest.

Data Availability Statement

The data that support the findings of this study are available from the corresponding author upon reasonable request.

Keywords: Chalcogens · Crystal Engineering · Cycloaddition · Selenocyanates · Topochemistry

[1] L. R. MacGillivray, G. S. Papaefstathiou, T. Friščić, T. D. Hamilton, D.-K. Bučar, Q. Chu, D. B. Varshney, I. G. Georgiev, *Acc. Chem. Res.* **2008**, *41*, 280–291.
[2] a) G. Campillo-Alvarado, C. Li, D. C. Swenson, L. R. MacGillivray, *Cryst. Growth Des.* **2019**, *19*, 2511–2518; b) E. Bosch, S. J. Kruse, H. R. Krueger, Jr., R. H. Groeneman, *Cryst. Growth Des.* **2019**, *19*, 3092–3096.
[3] a) D.-K. Bučar, A. Sen, S. V. S. Mariappan, L. R. MacGillivray, *Chem. Commun.* **2012**, *48*, 1790–1792; b) K. M. Hutchins, J. C. Sumrak, L. R. MacGillivray, *Org. Lett.* **2014**, *16*, 1052–1055; c) D. P. Ericson, Z. P. Zurfluh-Cunningham, R. H. Groeneman, E. Elacqua, E. W. Reinheimer, B. C. Noll, L. R. MacGillivray, *Cryst. Growth Des.* **2015**, *15*, 5744–5748; d) S. P. Yelgaonkar, D. C. Swenson, L. R. MacGillivray, *Chem. Sci.* **2020**, *11*, 3569–3573; e) D. B. Varshney, X. Gao, T. Friscic, L. R. MacGillivray, *Angew. Chem. Int. Ed.* **2006**, *45*, 646–650; *Angew. Chem.* **2006**, *118*, 662–666.
[4] a) C. Li, G. Campillo-Alvarado, D. C. Swenson, L. R. MacGillivray, *Inorg. Chem.* **2019**, *58*, 12497–12500; b) G. S. Papaefstathiou, Z. Zhong, L. Gang, L. R. MacGillivray, *J. Am. Chem. Soc.* **2004**, *126*, 9158–9159.
[5] a) T. Friščić, L. R. MacGillivray, *Z. Kristallogr.* **2005**, *220*, 351–363; b) I. Halasz, *Cryst. Growth Des.* **2010**, *10*, 2817–2823.
[6] G. M. J. Schmidt, *Pure Appl. Chem.* **1971**, *27*, 647–678.
[7] a) S. J. Kruse, E. Bosch, F. Brown, R. H. Groeneman, *Cryst. Growth Des.* **2020**, *20*, 1969–1974; b) M. A. Sinnwell, J. N. Blad, L. R. Thomas, L. R. MacGillivray, *IUCrJ* **2018**, *5*, 491–496; c) M. A. Sinnwell, L. R. MacGillivray, *Angew. Chem. Int. Ed.* **2016**, *55*, 3477–3480; *Angew. Chem.* **2016**, *128*, 3538–3541; d) T. Caronna, R. Liantonio, T. A. Logothetis, P. Metrangolo, T. Pilati, G. Resnati, *J. Am. Chem. Soc.* **2004**, *126*, 4500–4501; e) J. Quentin, D. C. Swenson, L. R. MacGillivray, *Molecules* **2020**, *25*, 907.
[8] a) P. Scilabra, G. Terraneo, G. Resnati, *Acc. Chem. Res.* **2019**, *52*, 1313–1324; b) L. Vogel, P. Wonner, S. M. Huber, *Angew. Chem. Int. Ed.* **2019**, *58*, 1880–1891; *Angew. Chem.* **2019**, *131*, 1896–1907.
[9] a) A. F. Cozzolino, J. F. Britten, I. Vargas-Baca, *Cryst. Growth Des.* **2006**, *6*, 181–186; b) A. F. Cozzolino, I. Vargas-Baca, S.

© 2022 The Authors. Angewandte Chemie International Edition published by Wiley-VCH GmbH

MOST WIEDZY Downloaded from mostwiedzy.pl

Mansour, A. H. Mahmoudkhani, *J. Am. Chem. Soc.* **2005**, *127*, 3184–3190; c) G. E. Garrett, G. L. Gibson, R. N. Straus, D. S. Seferos, M. S. Taylor, *J. Am. Chem. Soc.* **2015**, *137*, 4126–4133.
[10] P. C. Ho, P. Szydlowski, J. Sinclair, P. J. W. Elder, J. Kubel, C. Gendy, L. M. Lee, H. Jenkins, J. F. Britten, D. R. Morim, I. Vargas-Baca, *Nat. Commun.* **2016**, *7*, 11299.
[11] P. C. Ho, J. Rafique, J. Lee, L. M. Lee, H. A. Jenkins, J. F. Britten, A. L. Braga, I. Vargas-Baca, *Dalton Trans.* **2017**, *46*, 6570–6579.
[12] A. Kremer, A. Fermi, N. Biot, J. Wouters, D. Bonifazi, *Chem. Eur. J.* **2016**, *22*, 5665–5675.
[13] A. F. Cozzolino, Q. Yang, I. Vargas-Baca, *Cryst. Growth Des.* **2010**, *10*, 4959–4964.
[14] L.-J. Riwar, N. Trapp, K. Root, R. Zenobi, F. Diederich, *Angew. Chem. Int. Ed.* **2018**, *57*, 17259–17264; *Angew. Chem.* **2018**, *130*, 17506–17512.
[15] a) P. Wonner, L. Vogel, M. Dser, L. Gomes, F. Kniep, B. Mallick, D. B. Werz, S. M. Huber, *Angew. Chem. Int. Ed.* **2017**, *56*, 12009–12012; *Angew. Chem.* **2017**, *129*, 12172–12176; b) P. Wonner, L. Vogel, F. Kniep, S. M. Huber, *Chem. Eur. J.* **2017**, *23*, 16972–16975; c) P. Wonner, A. Dreger, L. Vogel, E. Engelage, S. M. Huber, *Angew. Chem. Int. Ed.* **2019**, *58*, 16923–16927; *Angew. Chem.* **2019**, *131*, 17079–17083; d) P. Wonner, T. Steinke, L. Vogel, S. M. Huber, *Chem. Eur. J.* **2020**, *26*, 1258–1262.
[16] S. Benz, A. I. Poblador-Bahamonde, N. Low-Ders, S. Matile, *Angew. Chem. Int. Ed.* **2018**, *57*, 5408–5412; *Angew. Chem.* **2018**, *130*, 5506–5510.
[17] M. S. Taylor, *Coord. Chem. Rev.* **2020**, *413*, 213270.
[18] N. A. Semenov, D. E. Gorbunov, M. V. Shakhova, G. E. Salnikov, I. Y. Bagryanskaya, V. V. Korolev, J. Beckmann, N. P. Gritsan, A. V. Zibarev, *Chem. Eur. J.* **2018**, *24*, 12983–12991.
[19] G. E. Garrett, E. I. Carrera, D. S. Seferos, M. S. Taylor, *Chem. Commun.* **2016**, *52*, 9881–9884.
[20] a) J. Y. C. Lim, I. Marques, A. L. Thompson, K. E. Christensen, V. Félix, P. D. Beer, *J. Am. Chem. Soc.* **2017**, *139*, 3122–3133; b) J. Y. C. Lim, J. Y. Liew, P. D. Beer, *Chem. Eur. J.* **2018**, *24*, 14560–14566; c) A. Borissov, I. Marques, J. Y. C. Lim, V. Félix, M. D. Smith, P. D. Beer, *J. Am. Chem. Soc.* **2019**, *141*, 4119–4129; d) J. Y. C. Lim, I. Marques, V. Félix, P. D. Beer, *Chem. Commun.* **2018**, *54*, 10851–10854.
[21] a) S. Benz, M. Macchione, Q. Verolet, J. Mareda, N. Sakai, S. Matile, *J. Am. Chem. Soc.* **2016**, *138*, 9093–9096; b) K. Strakova, L. Assies, A. Goujon, F. Piazzolla, H. V. Humeniuk, S. Matile, *Chem. Rev.* **2019**, *119*, 10977–11005; c) L. M. Lee, M. Tsemperouli, A. I. Poblador-Bahamonde, S. Benz, N. Sakai, K. Sugihara, S. Matile, *J. Am. Chem. Soc.* **2019**, *141*, 810–814.
[22] A. M. S. Riel, H.-T. Huynh, O. Jeannin, O. Berryman, M. Fourmigué, *Cryst. Growth Des.* **2019**, *19*, 1418–1425.
[23] A. Dhaka, O. Jeannin, I.-R. Jeon, E. Aubert, E. Espinosa, M. Fourmigué, *Angew. Chem. Int. Ed.* **2020**, *59*, 23583–23587; *Angew. Chem.* **2020**, *132*, 23789–23793.
[24] A. Dhaka, O. Jeannin, E. Aubert, E. Espinosa, M. Fourmigué, *Molecules* **2021**, *26*, 4050.
[25] H.-T. Huynh, O. Jeannin, M. Fourmigué, *Chem. Commun.* **2017**, *53*, 8467–8469.
[26] P. Nikolaienko, M. Rueping, *Chem. Eur. J.* **2016**, *22*, 2620–2623.
[27] Y. Guan, S. D. Townsend, *Org. Lett.* **2017**, *19*, 5252–5255.
[28] S. Redon, A. R. O. Kosso, J. Broggi, P. Vanelle, *Synthesis* **2019**, *51*, 3758–3765.
[29] X. Zhang, X.-B. Huang, Y.-B. Zhou, M.-C. Liu, H.-Y. Wu, *Chem. Eur. J.* **2021**, *27*, 944–948.
[30] a) K. Durka, K. N. Jarzembska, R. Kaminski, S. Lulinski, J. Serwatowski, K. Wozniak, *Cryst. Growth Des.* **2013**, *13*, 4181–4185; b) O. Seven, M. Bolte, H.-W. Lerner, M. Wagner, *Organometallics* **2014**, *33*, 1291–1299.
[31] a) O. Jeannin, H.-T. Huynh, A. M. S. Riel, M. Fourmigué, *New J. Chem.* **2018**, *42*, 10502–10509, and references therein; b) H.-T. Huynh, O. Jeannin, M. Fourmigué, *New J. Chem.* **2021**, *45*, 76–84.
[32] V. Kumar, C. Leroy, D. L. Bryce, *CrystEngComm* **2018**, *20*, 6406–6411.
[33] J. Stojaković, A. M. Whitis, L. R. MacGillivray, *Angew. Chem. Int. Ed.* **2013**, *52*, 12127–12130; *Angew. Chem.* **2013**, *125*, 12349–12352.
[34] Deposition Numbers 2168861, 2168862, 2168863, 2168864, 2168865, 2168866, 2168867, and 2168868 contain the supplementary crystallographic data for this paper. These data are provided free of charge by the joint Cambridge Crystallographic Data Centre and Fachinformationszentrum Karlsruhe Access Structures service.

Manuscript received: April 28, 2022
Accepted manuscript online: July 7, 2022
Version of record online: July 27, 2022

MOST WIEDZY Downloaded from mostwiedzy.pl

© 2022 The Authors. Angewandte Chemie International Edition published by Wiley-VCH GmbH